

A HIGH-PRECISION, HIGH-RELIABILITY BINARY ROTARY ENCODER USING HALL-EFFECT SENSORS

Sebastian Kottmeier⁽¹⁾, Silvio Müller⁽¹⁾, Tilo Schmidt⁽¹⁾, Kai Zajac⁽¹⁾, Matthias Schmalbach⁽²⁾

⁽¹⁾ Hoch Technologie Systeme GmbH, Am Glaswerk 6, 01640 Coswig, Germany, Email: info@htsdd.de

⁽²⁾ RUAG Schweiz AG, RUAG Space, Schaffhauserstrasse 580, 8052 Zürich, Switzerland, Email: Matthias.Schmalbach@ruag.com

ABSTRACT

The development of movable high precision optical instruments for space applications makes great demands on position measurement and control. The precise control of the spatial orientation of an optical component, such as mirrors or slit assemblies, with uncompromising reliability, requires specific solutions. The combined usage of high reliability hall-effect sensors and highly radiation resistant samarium-cobalt permanent magnets in a non-contact rotary position encoder provided a solution for a rotating mirror wheel with three stop positions. The fully redundant position sensing system was aimed to a mass below 75 g. As investigations have shown, further developments will allow turning the specific construction into a general purpose position encoding system.

1. INTRODUCTION

The Shutter/Calibration Mechanism (SCM) used in the Hyperspectral Imager of the Environmental Mapping and Analysis Program¹ (EnMAP) utilizes a rotating set of optical planes to control the optical path of the imagers' telescope.

Existing solutions, like small single-turn rotary encoders applied to the actuator gear shaft, do not offer the necessary precision, while incremental encoders may lose the absolute position information in case of malfunctions. Furthermore both techniques are accompanied by a vast amount of interpretation hardware, which in addition has to be qualified for

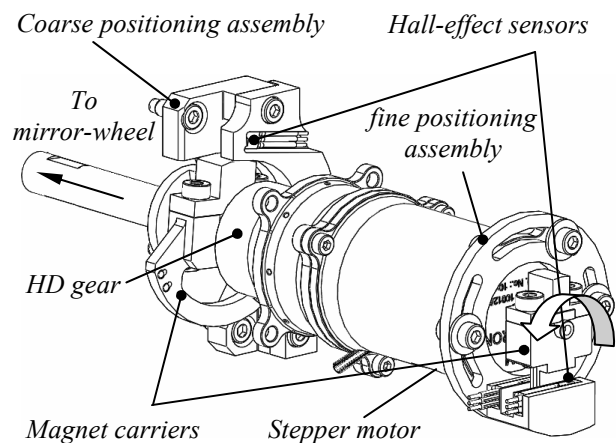


Figure 1: Principal setup of the encoder system.

space applications. To prevent the disadvantages of the mentioned solutions, the paper will describe a highly precise, cost effective; hall-sensor-trigger based motor encoder. The presented encoder can be used to rotate components to predefined operating points while returning a set of simple, Gray-code based TTL signals.

2. APPROACH

The actuator used for the shaft rotation and positioning is a unit consisting of a stepper motor and harmonic drive (HD) gear. The leading idea for building the rotary encoder is the segmentation into coarse- and fine-pointing components by the actuators HD gear. The coarse positioning assembly will act like a low resolution single turn encoder returning the actuator shaft position as binary coded signal from a set of sensors, one for each operating point. After the shaft position is determined by the coarse positioning

¹ Project of the German Aerospace Center (DLR FKZ 50 EP 0801)

assembly, the stepper motor will be rotated until the fine position assembly reaches its defined position (Figure 1). The precision is limited by the gear accuracy, the motor error and the precision of the hall-effect sensors.

2.1 Requirements

The system shall rotate a mirror wheel to three operating positions while maintaining a positioning accuracy of ± 1 arc minutes. The initial calibration accuracy has to be ± 5 arc minutes. The operational temperature is $21\text{ }^{\circ}\text{C} \pm 1\text{ K}$; the survival temperature range is $-50\text{ }^{\circ}\text{C}$ to $+80\text{ }^{\circ}\text{C}$. The mechanical loads are assessed to 70 g sine and 200 g shock in all dimensions. Figure 2 shows the critical mirror wheel positions, which are distributed equally around the perimeter.

2.2 Material

As technological basis for the development the combined use of a cylindrical Samarium-Cobalt Magnet ($\text{Sm}_2\text{Co}_{17}$, $\text{Ø}1,5\text{mm} \times 3\text{mm}$) and an OPTEK Technology OMH 30XX-series unipolar non-latching Hall-trigger is set. Samarium-Cobalt magnets are characterized through outstanding radiation hardness and chemical resistance [1], which make them suitable for space applications.

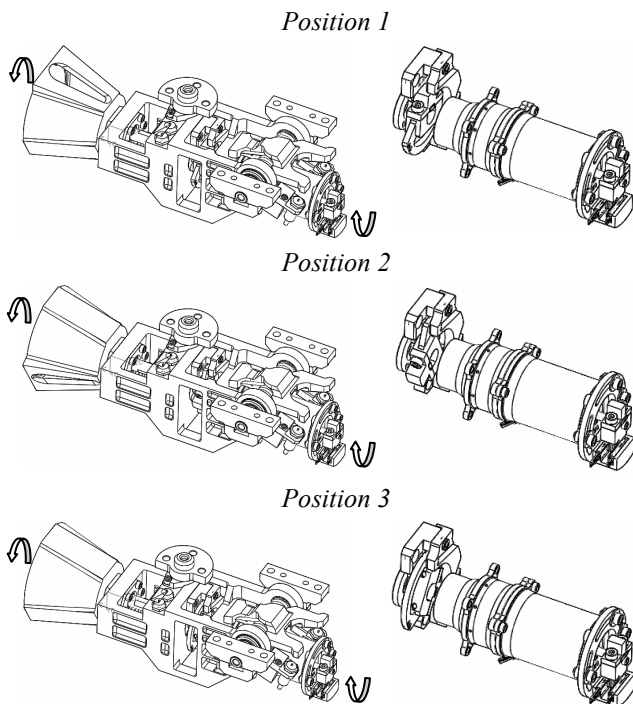


Figure 2: Mirror wheel positions of the SCM

The hall-effect sensors of the OPTEK OMH-Series are available as both MIL-STD-883 military (B-Grade) and space (S-Grade) qualified, whereupon the military grade components shall be used to reduce costs. The sensors circuitry contains a sensitive hall-element as well as a Schmitt trigger, what gives it the ability to switch between two defined output states depending on the faced magnetic flux density. The actuator consists of a hybrid stepper motor with a stepping angle of 1.8° and an attached 1:100 HD gear.

2.3 Encoding principle

To encode the three operational positions, a minimum of three sensors is needed. A coarse position detector, consisting of two magnet/ hall-sensor-pairs (two bit), is mounted on the gear shaft, while a fine position detector, consisting of one magnet/ hall-sensor-pair, is mounted on the second motor shaft (Figure 3).

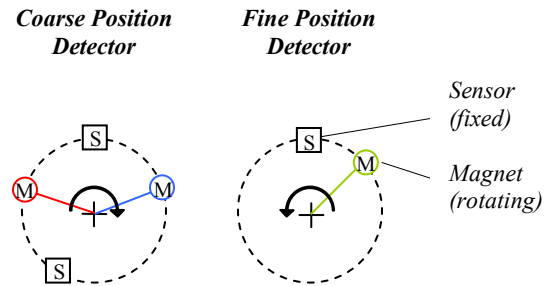


Figure 3: Encoder principle

Due to the gear, each motor step moves the gear shaft 1.08 arc minutes, what leads to a total of 20,000 steps needed for a full rotation. The logic states realized with the described setup are given in Table 1. The two sensors of the coarse position detector are called “A” and “B”.

Coarse A	Coarse B	Fine	Operational Position		
			1	2	3
0	0	0 / 1	0	0	0
1	0	1	1	0	0
1	1	1	0	1	0
0	1	1	0	0	1

Table 1: Logic states of the encoder system.

It has to be noted, that the “two bit / one bit” requires the angle between two operational positions to be a multiple of 200 steps. In all other cases more sensors are needed on the fine position detector. Equation 1

and Figure 4 show the relationship between the number of CPD sensors (n) and the encodable positions (p) in a “ n bit / one bit” system.

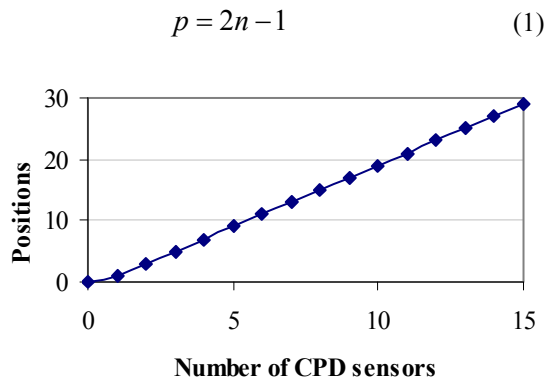


Figure 4: Relation between number of sensors and encodable positions

2.4 Sensor-magnet interaction

To develop a robust control unit, it is necessary to determine the physical and geometrical effects prevailing during the interaction of sensor and rotating magnetic field.

Figure 5 shows the principal mode of operation for a Hall-Sensor based trigger crossing the unaffected magnetic field of a SmCo-based permanent magnet.

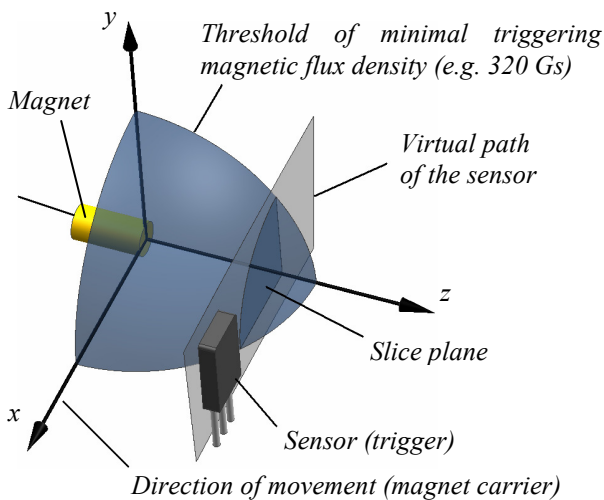


Figure 5: Principle of a Hall-sensor based encoder with laid in coordinate system

When the sensor passes the threshold-plane of its predefined switching flux density, it will change its logic state (in the described case the output voltage

drops from +5 V to 0 V). After switching his state, the sensor will face a second threshold plane because of the implemented hysteresis. The crossing of the second plane will lead to a reset of the output state. Additionally, the sensor will only change its output state when facing a magnetic south pole, what will become important in redundant design. It is obvious, that the geometry of the slice plane along the sensors path is to complex to be used in the initial design process and has to be replaced by a more tangible term. Therefore, all calculations will only consider the virtual path of the center point of the sensors hall element, what reduces the problem in a way given in Figure 6, if the diameter of the magnet carrier is much larger than the length of the path. With this assumption, the number of steps needed to pass through the triggered state can be easily approximated as arc length.

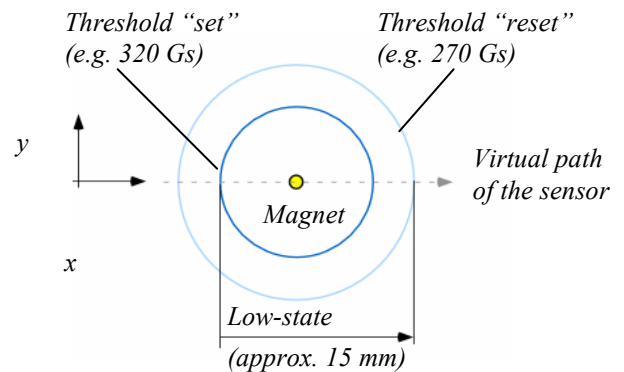


Figure 6: Path of the center of the hall element

2.5 Signal geometry

It becomes apparent, that the precision of this sensor system depends on the following parameters:

- The geometry of the magnetic field, i.e. the geometry of the threshold plane.
- The geometry and spatial orientation of the actual sensitive element inside the hall-sensors case.
- The sensitivity of the hall-element and the trigger circuit, i.e. the integral magnetic flux normal to the sensitive surface necessary to trigger the signal.
- The mechanical precision and manufacturing tolerances of the sensor- and magnet carriers as well as the precision of the motor and gear.

These parameters influence the geometry and materials of the encoder hardware as well as the relationship between the motor steps and the geometry of the electrical signals.

Due to the geometrical limitations resulting from the design of the SCM structure the air gap between magnet and sensor surface is set to 0.5 mm, what gives a starting point for the electromagnetic simulation. To generate a proper FEA-model, the magnetic flux density along the virtual sensor path had to be surveyed utilizing a magnetometer.

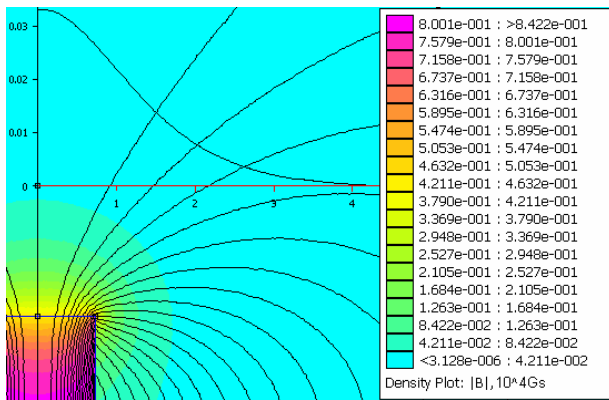


Figure 7: FE-model of the $\text{Sm}_2\text{Co}_{17}$ magnet with the overlaid curve progression of the flux density along the air gap.

The FEA-model (Figure 7) was then used to determine the effects of the triggers hysteresis on the virtual path of the sensor. This is crucial as the limited air gap may cause the triggered state to last for more than one motor step, depending on the physical parameters of sensor and magnet. In combination with the information about the sensor hysteresis, the FEA-data can be used to simulate the geometry of the three signals, including errors depending on the factors mentioned above. Furthermore the geometry of the mechanical components can be optimized. Figure 8 shows an idealized detail of the generated signal diagram: After a change in output states of the coarse position detector the fine position detector indicates the calibrated position. Due to imperfections in manufacturing the coarse position signals will not change their state at the same position. To gain unique output states in the described configuration, it has to be guaranteed, that the coarse signals will not last longer than 399 steps and include more than 1 fine signal.

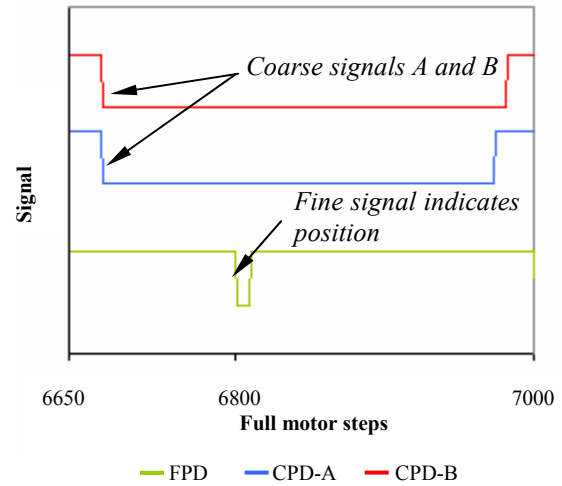


Figure 8: Signal diagram detail (idealized) of position 2

2.5 Encoder design and redundancy

The fine positioning sensor carrier as shown Figure 9 is flanged to the stepper motor and has two separated slots to hold the nominal and redundant hall trigger. Three slotted holes permit the rotation of the sensor carrier for the initial calibration. The magnet carrier holds two cylindrical $\text{Sm}_2\text{Co}_{17}$ magnets, each facing with its south pole to the respective sensor in order to realize the redundancy. The magnet carrier is locked against distortion.

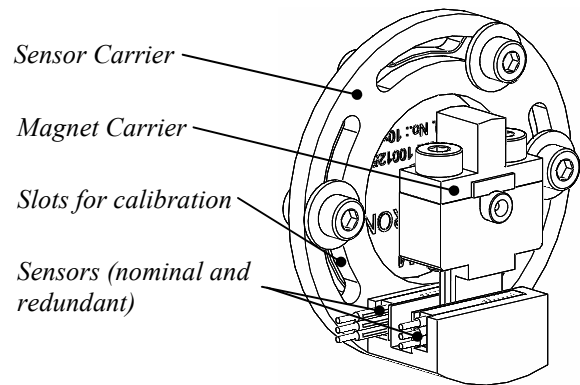


Figure 9: Fine position detector

The coarse position detector (Figure 10) consists of two sensor carriers each for nominal and redundant side, which are mounted to the SCM structure. A centering device adjusts the alignment of the nominal sensor carrier. A relatively coarse borehole clearance allows a slight correction of the carrier position in order to calibrate the system. The magnet carrier is mounted on a flattening on the actuator gear shaft.

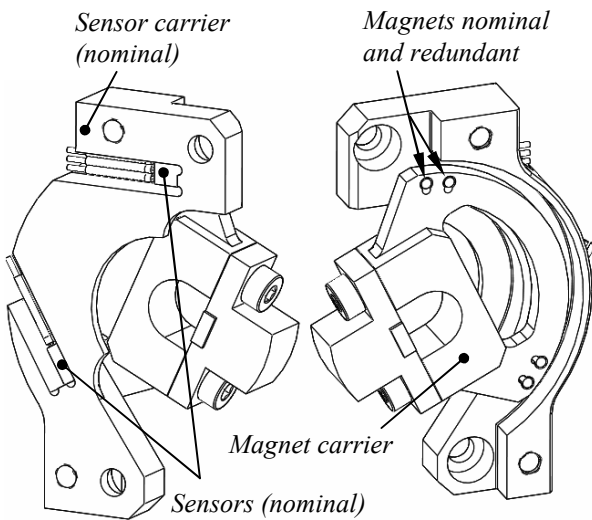


Figure 10: Coarse position detector, redundant sensor carrier removed

As in the fine position detector, the nominal and redundant side have an angular offset to minimize the interaction of the magnetic fields.

2.6 Degradation

In the described case it has to be assured, that a possible degradation of the hall sensors sensitivity due to radiation effects does not cause a loss of steps at the fine position detector. Therefore, the maximum allowable drift in the trigger point position is 0.9° for a

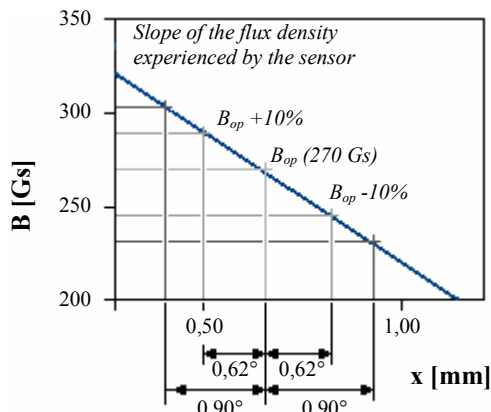


Figure 11: Possible effects for a given 10% degradation of the triggering flux density for the fine position detection

stepping motor with a stepping angle of 1.8° . Figure 11 shows the geometrical impact of a shift in the

triggering flux density derived from the FEA-model: For a given encoder wheel with a diameter of 15 mm a drift of $\pm 10\%$ causes the geometrical trigger point to move about 0.6° along the perimeter of the fine pointing encoder. As tests have shown, the dose necessary for a 10% drift lays above 40 krad [2] for a similar sensor, while the received dose during the mission time is estimated with a maximum of 11 krad.

3 Breadboard tests

To determine the systems functionality, two parameters had to be analyzed:

- *The initial calibration accuracy*
- *The repeatable positioning accuracy*

To measure the maximum possible accuracy of the sensor system, a breadboard has been developed.

The test is designed to resemble the geometrical and mechanical parameters of the SCM while allowing the measurement of the position of the wheel. The breadboard consists of an electrically and mechanically equivalent stepper motor with attached coarse- and fine position detectors, flanged to a geometry dummy of the SCM structure. To measure the angular deviation of the reached position, the breadboard utilizes a mirror dummy in combination with two Keyence LK-G 82 laser distance sensors. Both sensors measure the distance to the mirror dummies surface.

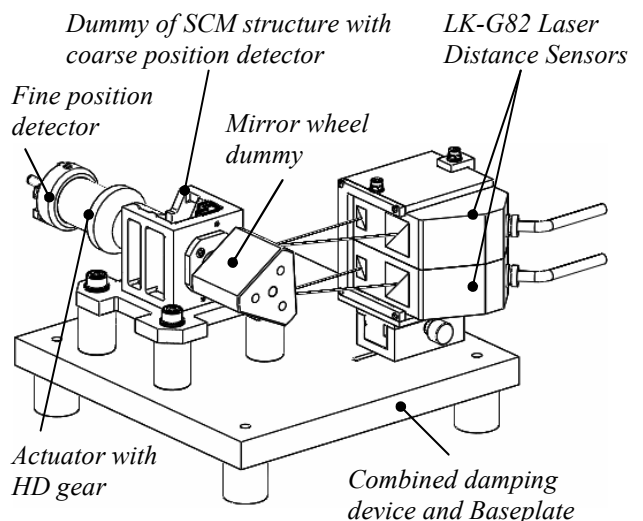


Figure 12: Sensor system breadboard

With the known clearance between the laser dots the angular displacement of the mirror dummy can be triangulated:

$$\kappa = \arctan\left(\frac{D_1 - D_2}{\lambda}\right) = \arctan\left(\frac{A}{\lambda}\right) \quad (2)$$

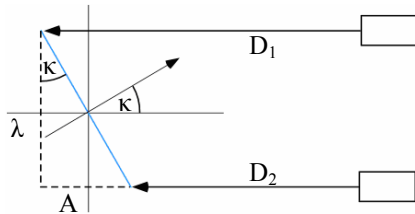


Figure 13: Principle of deviation detection

In full step mode the detectable angle has to be smaller than 1.08 arc minutes to fulfill the requirements. The maximal resolution of the laser distance sensors is 0.2 μm, what, with the given geometry, results in a maximum angular resolution of $6.4 \cdot 10^{-4}$ (0,038 arc minutes). Resulting from this accuracy, the stepping mode of the actuator can be set to 1/10 step for optimal accuracy at the angular measurements.

The breadboard test consists of three consecutive phases.

A. Calibration of the laser distance sensors to the coordinate system of the breadboard baseplate by measuring the distance offset via a reference plane.

B. Measuring the absolute angular deviation of the mirror after position 1 is reached.

C. Repeating search for position 1 to determine the repositioning accuracy.

Phase C. will show the absolute positioning accuracy of the whole encoder system, including all mechanical parts. Therefore the actuator will rotate the mirror wheel dummy 19950 full steps before switching to 1/10 step mode. Then the sensor system will gain control over the actuator by searching for the coarse position signals resembling position 2. After both signals are active, the next occurring fine position detector signal is searched and the angular deviation of the mirror wheel dummy is measured. This operation is repeated until a sufficient number of samples is reached.

To minimize effects caused by thermal elongation the environmental temperature will be automatically regulated to $21 \text{ °C} \pm 1 \text{ K}$ via a temperature sensor mounted on the encoders gear housing. Errors from torsion or bending will be compensated by proper pausing intervals after reaching the defined position. Degradation effects caused by radiation or heat cycles have not been determined but could have impact on the long-term precision of the system.

4 RESULTS

The conducted test has shown a high angular accuracy. Figure 14 shows the results of test phase C. The measured distances are the mean values of 100,000 samples per point gained over a period of 10 seconds to minimize effects caused by vibrations. The results were then normalised to the measurements average to clarify the maximal deviation. As can be seen, the samples fluctuate in a ± 0.12 arc minute interval at a given mean measurement error of 0.0136 arc minutes. In an adjacent test, the reduction of

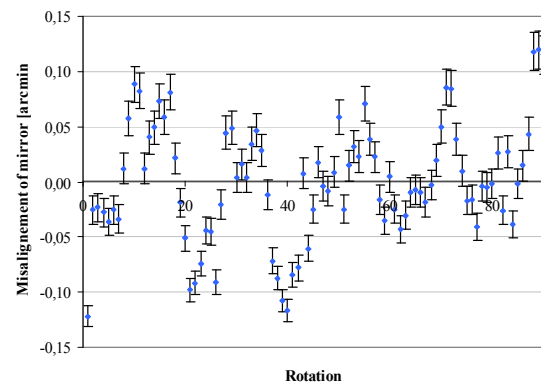


Figure 14: Angular deviation in test phase C

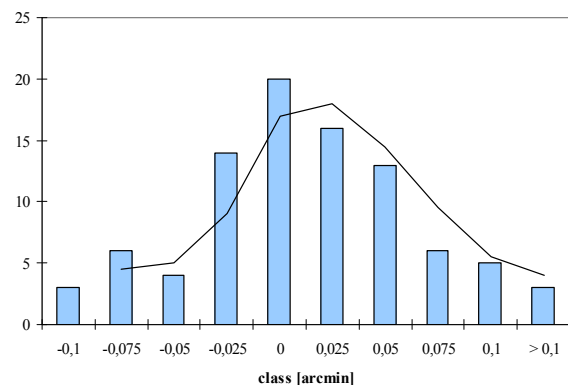


Figure 15: Angular deviation histogram function

the stepping mode to 1/256 does not significantly enhance the acquirable accuracy. Transferring the data into a histogram function (Figure 15) shows that the deviation is distributed normally around the mean value, except a glitch in the -0.05-class. To decide whether this is an irregularity following the sample size or a physical effect has to be determined in further examinations. The sample distribution and the curve progression do not show any drift but there seems to be a slight correlation to the surrounding temperature (Figure 16). Whether this effect is caused by a shift in sensitivity or mechanical elongation can not be inferred from the given data.

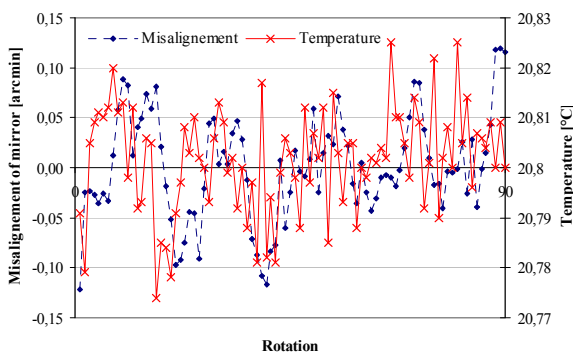


Figure 16: Correlation between misalignment and temperature

5 LESSONS LEARNT

- Hall effect trigger thresholds scatter widely around the given mean value, even if the sensors are from the same production batch. When used in high precision applications, it is necessary to measure the exact trigger point for every deployed sensor.
- The same problem appears for permanent magnets due to the composition of the alloy. For FEA-modeling the remanence has to be determined through testing.
- The MIL-STD-883-B grade hall-effect triggers have been qualified for this specific task with an additional destructive physical analysis (DPA) test.

6 CONCLUSION

A non-contact rotary encoder utilizing hall-effect sensors has been developed to control the spatial orientation of an optical satellite mechanism.

Breadboard tests have proven the usability and high precision of the proposed rotary encoder within the given requirements. The actuator gear in combination with the encoder signal system ensures a repeatable resolution of about 0.12 arc minutes. The mass of a system consisting of six sensors (three nominal and redundant each) to encode three operating positions stays below 40 g.

Further investigations will include long-term performance, thermal-vacuum, thermal cycling and vibration tests and their effect on the absolute angular precision of the calibrated system. Furthermore a test of the absolute precision in a regulated thermal environment may clarify the relationship between misalignment and temperature.

7 ABBREVIATIONS AND ACRONYMS

CPD	Coarse Position Detector
EnMAP	Environmental Mapping and Analysis Program
FEA	Finite element analysis
FPD	Fine Position Detector
HD	Harmonic Drive
op	Operating Point
rp	Reset Point
SCM	Shutter / Calibration Mechanism
TTL	Transistor-transistor logic

A	m	Differential distance
B	Gs	Magnetic Flux Density
D	m	Distance
κ	$^{\circ}$	Angular deviation
λ	m	Distance between laser dots

8 REFERENCES

1. Liu, Jinfang et. al. (2007). *Thermal stability and radiation resistance of Sm-Co based permanent magnets*. Proceedings of Space Nuclear Conference. Boston, USA.
2. A. B. Sanders, H. S. Kim, and A. Phan (2008). *TID and SEE Response of Optek Hall Effect Sensors*. Radiation Effects Data Workshop, IEEE, New Jersey, USA.